

해상풍력단지에서의 PMSG 풍력발전기를 활용한 계통연계점 불평형 전원 보상

강자윤¹, 한대수¹, 서용석[†], 정병창², 김정중², 박종형², 최영준²

Compensation of Unbalanced PCC Voltage in an Off-shore Wind Farm of PMSG Type Turbines

Ja-Yoon Kang¹, Dae-Su Han¹, Yong-Sug Suh[†], Byoung-Chang Jung², Jeong-Joong Kim²,
Jong-Hyung Park², and Young-Joon Choi²

Abstract

This paper proposes a control algorithm for permanent magnet synchronous generators with a back-to-back three-level neutral-point clamped voltage source converter in a medium-voltage off-shore wind power system under unbalanced grid conditions. Specifically, the proposed control algorithm compensates for unbalanced grid voltage at the PCC (Point of Common Coupling) in a collector bus of an off-shore wind power system. This control algorithm has been formulated based on symmetrical components in positive and negative synchronous rotating reference frames under generalized unbalanced operating conditions. Instantaneous active and reactive power is described in terms of symmetrical components of measured grid input voltages and currents. Negative sequential component of AC input current is injected into the PCC in the proposed control strategy. The amplitude of negative sequential component is calculated to minimize the negative sequential component of grid voltage under the limitation of current capability in a voltage source converter. The proposed control algorithm enables the provision of balanced voltage at the PCC resulting in the high quality generated power from off-shore wind power systems under unbalanced network conditions.

Key words: Unbalanced grid, PCC, PMSG, Converter, Wind power system, Negative sequence current

1. Introduction

Wind power system is one of the fastest growing renewable energy systems. Wind power installation has been increasing both in number and size of individual wind turbine unit. In large scaled MW-range wind turbines, PMSG (Permanent Magnet Synchronous Generator) type wind turbine involving a

full-scaled PCS (Power Conditioning System) becomes a dominant choice due to its superb performance in active and reactive power generation.

Recently, grid codes about LVRT and operation under unbalanced grid become very strict. In general, unbalanced current is caused by unbalanced grid conditions, and it leads to unbalanced voltage at PCC (Point of Common Coupling). These unbalanced voltage conditions generate ripple and distortion of dc-link and grid current^[1]. Most of previous studies regarding unbalanced grid input focused on stabilizing the operation of wind turbine PCS itself, i.e. reducing the harmonics in ac input current and dc-link voltage, or compensating unbalanced grid current^{[1],[2]}. There have been several studies trying to solve unbalanced PCC problem instead of PCS itself. Some papers proposed a compensating solution employing an

Paper number: TKPE-2015-20-1-1

Print ISSN: 1229-2214 Online ISSN: 2288-6281

[†] Corresponding author: ysuh@jbnu.ac.kr, Dept. of Electrical Eng., Smart Grid Research Center, Chonbuk National University, Korea

Tel: +82-63-270-3381 Fax: +82-63-270-3381

¹ Dept. of Electrical Eng., Smart Grid Research Center, Chonbuk National University, Korea

² Power & Industrial Systems R&D Center, Hyosung Co.

Manuscript received Aug. 7, 2014; accepted Oct. 20, 2014

— 본 논문은 2014년 전력전자학술대회 우수추천논문임

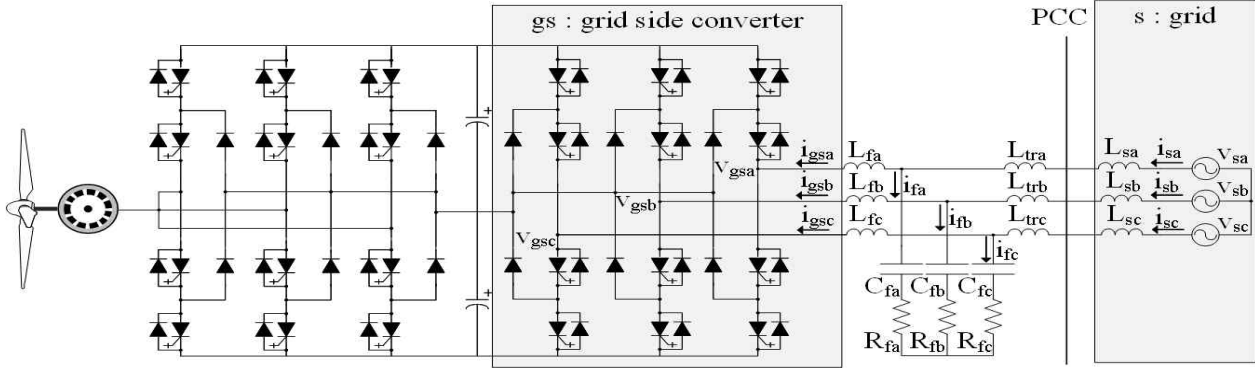


Fig. 1. PMSG wind turbine with a back-to-back 3-level NPC VSC.

additional active power filter at PCC^[3]. Other papers proposed compensation for unbalanced voltage at PCC using STATCOM^[4]. There has been a little work dealing with unbalanced PCC problem solely by PCS itself without employing additional active power filter or STATCOM.

This paper proposes a control algorithm to actively compensate for the unbalanced grid voltage at PCC. Negative sequence current is injected to the grid to cancel the negative sequential component of grid voltage at PCC. The amplitude of injected negative sequence current is computed under the limit of maximum input current of PCS. Negative sequential component of input current is regulated separately in the clockwise-rotating synchronous reference frame irrespective of positive sequential component of input current. Proposed control algorithm performs under the current capability limit of PCS and also improves the quality of output power from wind farm. Detailed calculation result as well as simulation and experiment result of 2.7MW wind turbine of PMSG type is provided to validate the proposed control algorithm in this paper. This paper is structured as follows. In Section 2, the modeling of PMSG is constructed under unbalanced grid. Section 3 describes the imbalance factor. Proposed control algorithm is explained in Section 4. Finally, Section 5 and 6 provide the simulation and experimental result to validate the proposed control algorithm, respectively.

2. Modeling of PMSG under Unbalanced Grid

Under unbalanced grid voltage, PMSG can be effectively modeled by using both positive and negative sequence components of voltages and currents in grid-side converter and input filter as shown in Fig. 1. The positive and negative sequence

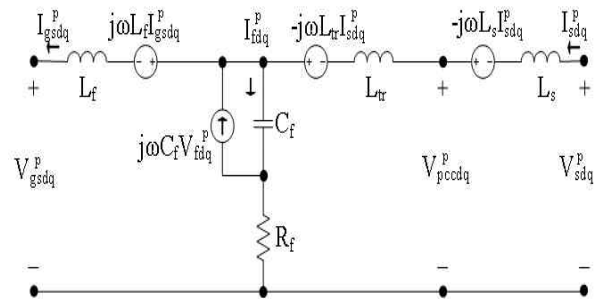


Fig. 2. Equivalent circuit of positive sequence dq components in CCW-rotating synchronous reference frame.

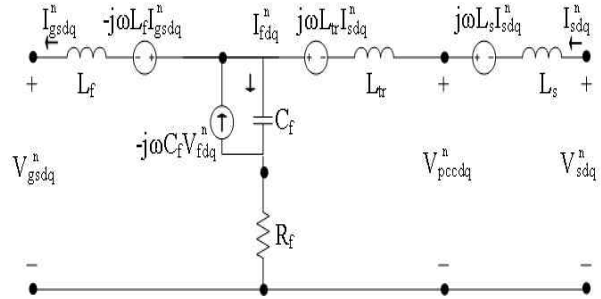


Fig. 3. Equivalent circuit of negative sequence dq components in CW-rotating synchronous reference frame.

components in a CCW-rotating and CW-rotating synchronous reference frame, respectively, are expressed as followings;

$$V_{gsd}^p - \omega L_f I_{gsq}^p + L_f \frac{d}{dt} I_{gsd}^p = V_{sd}^p + \omega (L_{tr} + L_s) I_{sq}^p - (L_{tr} + L_s) \frac{d}{dt} I_{sd}^p \quad (1)$$

$$-\omega C_f V_{fdq}^p + C_f \frac{d}{dt} V_{fdq}^p = I_{sd}^p - I_{gsd}^p \quad (2)$$

$$V_{gsd}^n + \omega L_f I_{gsd}^n + L_f \frac{d}{dt} I_{gsq}^n = V_{sq}^n - \omega (L_{tr} + L_s) I_{sd}^n - (L_{tr} + L_s) \frac{d}{dt} I_{sq}^n \quad (3)$$

$$\omega C_f V_{fd}^p + C_f \frac{d}{dt} V_{fq}^p = I_{sq}^p - I_{gsq}^p \quad (4)$$

$$V_{gsd}^n + \omega L_f I_{gsq}^n + L_f \frac{d}{dt} I_{gsd}^n = V_{sd}^n - \omega(L_{tr} + L_s) I_{sq}^n - (L_{tr} + L_s) \frac{d}{dt} I_{sd}^n \quad (5)$$

$$\omega C_f V_{fd}^n + C_f \frac{d}{dt} V_{fq}^n = I_{sd}^n - I_{gsd}^n \quad (6)$$

$$V_{gsq}^n - \omega L_f I_{gsd}^n + L_f \frac{d}{dt} I_{gsq}^n = V_{sq}^n + \omega(L_{tr} + L_s) I_{sd}^n - (L_{tr} + L_s) \frac{d}{dt} I_{sq}^n \quad (7)$$

$$-\omega C_f V_{fd}^n + C_f \frac{d}{dt} V_{fq}^n = I_{sq}^n - I_{gsq}^n \quad (8)$$

Based on the model given in (1)–(8), the equivalent circuit of grid input side of PMSG corresponding to positive and negative sequential components can be generated as shown in Fig. 2 and 3.

3. Imbalance Factor

Imbalance Factor (IF) is a metric factor describing the depth of imbalance. In this paper, *IF* is newly defined to be the ratio of magnitude of negative sequence to that of positive sequence component as shown in (9). Imbalance depth of grid and PCC voltage are quantitatively expressed employing a newly defined *IF* in this paper. In general, imbalance type is classified into four different cases as shown in TABLE I. The newly defined *IF* can effectively describe the depth of imbalance in all four cases. As an example, the correlation of newly defined *IF* and the per unit value of single-phase voltage sag of Type B are given in TABLE II.

$$IF = \sqrt{\frac{(V_{sd}^n)^2 + (V_{sq}^n)^2}{(V_{sd}^p)^2 + (V_{sq}^p)^2}} \quad (9)$$

4. Negative-sequence Current Injection (NCI) Control Algorithm

4.1 Calculation of Reference Current

This paper proposes Negative-sequence Current Injection (NCI) algorithm to actively compensate for the imbalance of PCC voltage by controlling negative sequence current. Balanced PCC voltage implies that the negative sequential components of corresponding voltage must be zero. Negative sequential components of ac input current (I_{sd}^n and I_{sq}^n) are regulated, in other words, injected to the grid in such a way that

TABLE I
IMBALANCE TYPE

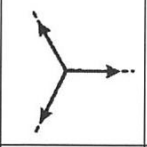
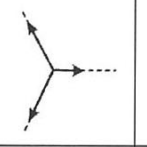
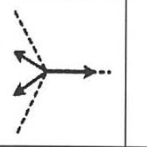
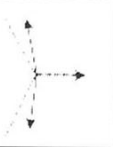
			
Type A	Type B	Type C	Type D
Voltage sag of three-phase	Voltage sag of single-phase	Single line-ground fault in Δ -Y transformer	Double line-ground fault in Δ -Y transformer

TABLE II
IF ACCORDING TO IMBALANCE DEGREE OF TYPE B

Voltage sag (pu)	1	0.9	0.8	0.7	0.6	0.5	0.3	0.1
IF (%)	0	3	7	11	15	20	30	43

the negative sequential components of PCC voltage (V_{pccd}^n and V_{pccq}^n) are cancelled.

In general, ac input current regulator requires four current references (I_{sd}^p , I_{sq}^p , I_{sd}^n , and I_{sq}^n). These four current reference values are calculated to meet certain control strategies. In this paper, four control strategies are formulated to satisfy the balanced PCC voltage and active/reactive power generation conditions.

First and second control strategies are to keep balanced PCC voltage. In Fig. 2 and 3, the negative sequential components of ac input current (I_{sd}^n and I_{sq}^n) are related with the negative sequential components of PCC voltage (V_{pccd}^n and V_{pccq}^n) as the following;

$$I_{sq}^n = \frac{V_{sd}^n - V_{pccd}^n}{\omega L_s} \quad (10)$$

$$I_{sd}^n = -\frac{V_{sq}^n - V_{pccq}^n}{\omega L_s} \quad (11)$$

If V_{pccd}^n and V_{pccq}^n are to be zero, then I_{sd}^n and I_{sq}^n are simplified as in (12) and (13).

$$I_{sq}^n = \frac{V_{sd}^n}{\omega L_s} \quad (12)$$

$$I_{sd}^n = -\frac{V_{sq}^n}{\omega L_s} \quad (13)$$

The third and fourth control strategies are to meet the demand of active and reactive power generation. The average values of instantaneous input active and

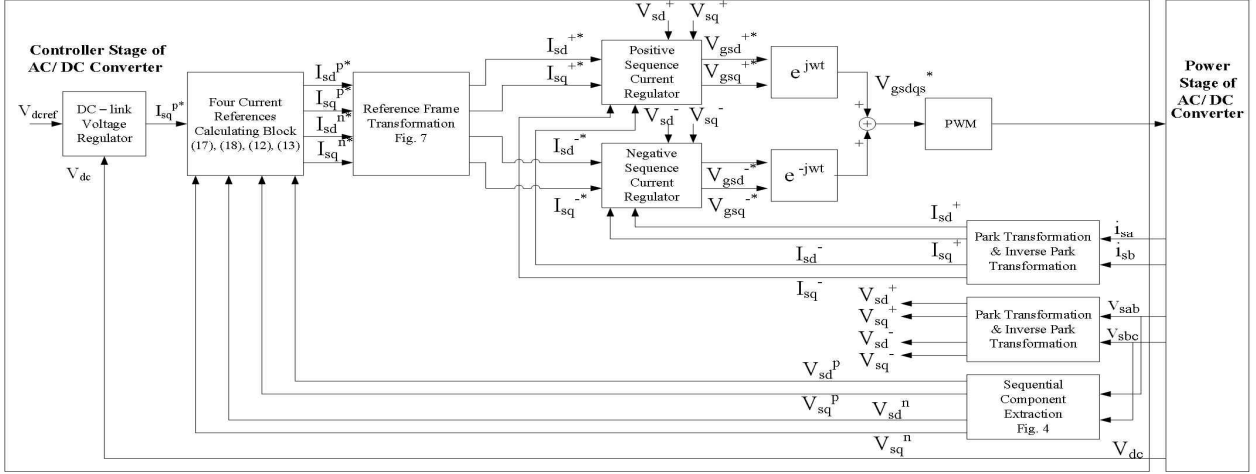


Fig. 4. Overall control block diagram.

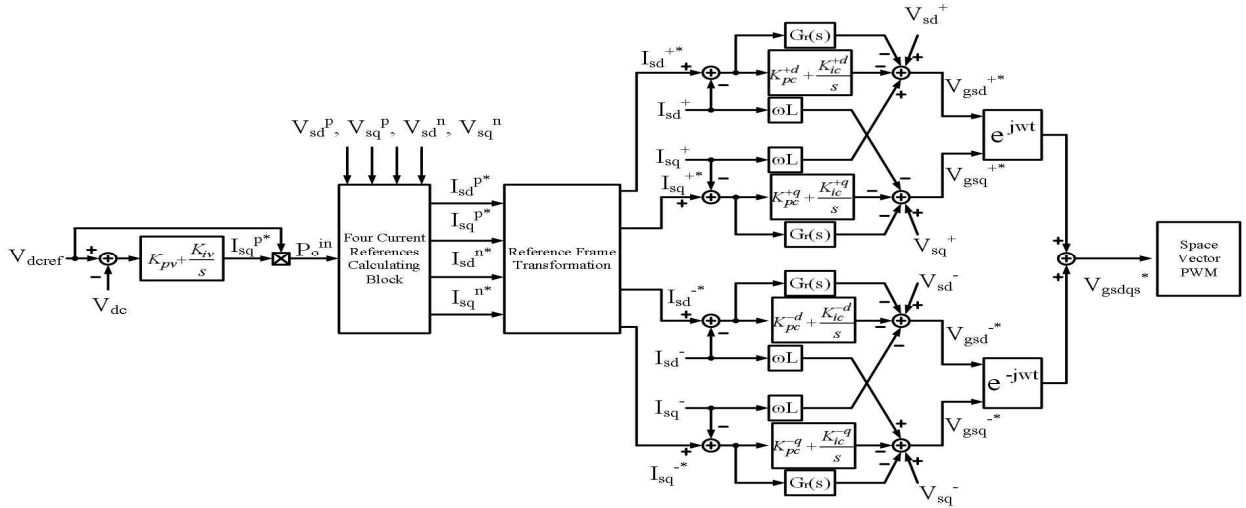


Fig. 5. Detailed control block diagram of dual frame current regulator.

reactive power can be formulated in terms of sequential components of ac input voltage and current as followings.

$$\frac{2}{3} P_{so} = V_{sd}^p I_{sd}^p + V_{sq}^p I_{sq}^p + V_{sd}^n I_{sd}^n + V_{sq}^n I_{sq}^n \quad (14)$$

$$\frac{2}{3} Q_{so} = V_{sq}^p I_{sd}^p - V_{sd}^p I_{sq}^p - V_{sq}^n I_{sd}^n + V_{sd}^n I_{sq}^n \quad (15)$$

After applying (12) and (13) into (14) and (15), rearranging terms lead to (16).

$$\frac{2}{3} \begin{bmatrix} P_{so} \\ Q_{so} \end{bmatrix} = \begin{bmatrix} V_{sd}^p & V_{sq}^p \\ V_{sq}^p & -V_{sd}^p \end{bmatrix} \begin{bmatrix} I_{sd}^p \\ I_{sq}^p \end{bmatrix} + \frac{1}{\omega L_s} \begin{bmatrix} V_{sd}^n & V_{sq}^n \\ -V_{sq}^n & V_{sd}^n \end{bmatrix} \begin{bmatrix} -V_{sd}^n \\ V_{sq}^n \end{bmatrix} \quad (16)$$

Finally I_{sd}^p and I_{sq}^p can be obtained from (16).

$$I_{sd}^p = \frac{2}{3} \frac{P_{so}}{(V_{sd}^p)^2 + (V_{sq}^p)^2} (V_{sd}^p + V_{sq}^p k_{pf}) - \frac{V_{sq}^p}{(V_{sd}^p)^2 + (V_{sq}^p)^2} \frac{(V_{sd}^n)^2 + (V_{sq}^n)^2}{\omega L_s} \quad (17)$$

$$I_{sq}^p = \frac{2}{3} \frac{P_{so}}{(V_{sd}^p)^2 + (V_{sq}^p)^2} (V_{sq}^p + V_{sd}^p k_{pf}) + \frac{V_{sd}^p}{(V_{sd}^p)^2 + (V_{sq}^p)^2} \frac{(V_{sd}^n)^2 + (V_{sq}^n)^2}{\omega L_s} \quad (18)$$

As a result, the positive and negative sequential components of ac input grid currents (I_{sd}^p , I_{sq}^p , I_{sd}^n , and I_{sq}^n) are calculated from four equations of (12), (13), (17), and (18). They are used as current reference values in a dual-frame current regulator^[2].

In (17) and (18), the new parameter of k_{pf} is employed. The parameter is defined as the ratio between the reactive power (Q_{so}) and active power

(P_{so}). Therefore, under the condition of unity power factor, i.e. zero value of Q_{so} , the parameter of k_{pf} is equal to zero. The relationship between the newly defined parameter k_{pf} and the classical power factor pf is described in (19).

$$k_{pf} = \frac{Q_{so}}{P_{so}} = \frac{\sqrt{1-pf^2}}{pf} \quad (19)$$

4.2 Control Block Diagram

The overall control structure consists of two nested regulating loops; the outer dc-link voltage regulating loop and the inner ac current regulating loop. The outer voltage regulating loop determines the reference signals for the inner current loop according to the four control strategies described in Section 4.1. The inner current loop is made up of two parallel dq synchronous frame current regulators; one for the positive sequence and the other for the negative sequence. Fig. 4 shows the entire control scheme block diagram.

A detailed control block diagram of the cascade dual current regulator with a voltage regulator is shown in Fig. 5. In general, it is required that the bandwidth of current regulation loop is high enough to maintain the fast dynamics of complete system. Sequence separation method of input current typically involves the low pass filter or notch filter to filter out the negative (positive) sequential component of twice input frequency in positive (negative) synchronous rotating reference frame. These low pass filter and notch filter in the current feedback path usually undermine the bandwidth of current regulation loop or phase margin of the system^[2]. In this paper, instead of separating the positive and negative sequence component from the total signal, these two components are rotated together in a counterclockwise direction to be regulated in a positive synchronous rotating reference frame and in a clockwise direction to be regulated in a negative synchronous rotating reference frame, respectively^[2]. The measured three-phase ac input current quantities are directly transformed to either positive or negative synchronous rotating reference frame resulting in the ac signal of twice line frequency imposed on the dc signal without being decomposed into separate positive and negative sequential components. However, the four current references that are calculated based on four control

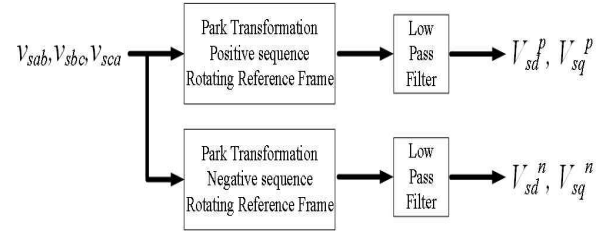


Fig. 6. Sequential component extraction block.

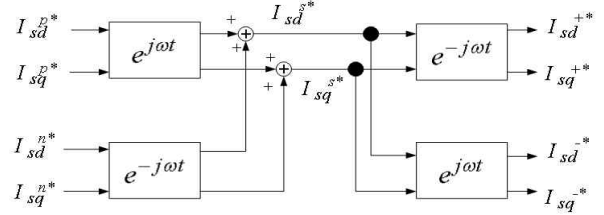


Fig. 7. Reference frame transformation block.

strategies are dc signals separated in positive/negative sequence synchronous rotating reference frames. Therefore, in order to match the calculated current reference values (I_{sd}^{p*} , I_{sq}^{p*} , I_{sd}^{n*} , and I_{sq}^{n*}) to measured current quantities (I_{sd}^p , I_{sq}^p , I_{sd}^n , and I_{sq}^n) in the same transformation frames, the reference values should be transformed accordingly.

The current regulator employed in this paper is dual-frame current regulator of [2]. The proposed control scheme features the current reference calculating block described by (12), (13), (17), and (18). This current reference calculating block for compensating unbalanced PCC voltage is shown in Fig. 4.

Figure 6 illustrates the computational process deriving the positive and negative sequence voltage component from the grid voltage in this paper. Measured value of grid voltage is transformed into a CCW and CW rotating reference frame of positive and negative sequence, respectively. Low pass filter is also used to filter out the opposite sequential component of twice line frequency.

In Fig. 7, the process of reference frame transformation is described. Mathematical description of output variables in terms of input variables are given in (20) – (23).

$$I_d^{+*} = I_d^{p*} + \cos(2\omega t) I_d^{n*} + \sin(2\omega t) I_q^{n*} \quad (20)$$

$$I_q^{+*} = I_q^{p*} + \cos(2\omega t) I_q^{n*} - \sin(2\omega t) I_d^{n*} \quad (21)$$

$$I_d^* = I_d^{n*} + \cos(2\omega t)I_d^{p*} - \sin(2\omega t)I_q^{p*} \quad (22)$$

$$I_q^* = I_q^{n*} + \cos(2\omega t)I_q^{p*} + \sin(2\omega t)I_d^{p*} \quad (23)$$

5. Simulation

The NCI control algorithm which is proposed in this paper is verified through the simulation. Parameters of PMSG employed in the simulation are summarized in TABLE III. In this paper simulation result is presented for the case of Type B unbalanced grid with the IF of 3%. Output power generated from wind turbine is assumed to be 60% of rated power.

Under the unbalanced grid and output power generation condition, the three-phase line voltages at PCC are illustrated in Fig. 8 and 9. Waveforms in Fig. 8 are obtained under the condition without NCI compensating algorithm being employed, i.e. the conventional single-frame current regulator of positive sequential component of ac input current only. Waveforms in Fig. 9 are obtained under the condition with NCI compensating algorithm being employed. It is noted from the frequency spectrum in Fig. 8 that the amplitudes of three-phase line voltages are unbalanced. The corresponding numerical data are summarized in TABLE IV for the sake of readers' convenience. In Fig. 8, the imbalance factor of line voltages at PCC is close to that of grid input voltages, i.e. IF=3%. As shown in Fig. 9 and TABLE IV, the proposed NCI control algorithm actively compensates for the unbalanced grid voltage. As a result NCI control algorithm makes the three-phase line voltages at PCC balanced having the IF of almost zero.

The compensation of unbalanced PCC voltage is made possible by the injection of negative sequence current to the grid. Fig. 10 provides the waveforms of three-phase ac input currents under the condition without NCI control algorithm being considered. Fig. 11 shows the waveforms of three-phase ac input currents under the condition with NCI control algorithm considered. It is clearly noted from Fig. 11 that the three-phase ac input currents become more unbalanced as compared to those of Fig. 10 because of injected negative sequential component of input current. The peak amplitude of input current at maximum is increased from 449A in Fig. 10 to 623A in Fig. 11. This increase of amplitude of ac input current

TABLE III
PARAMETERS OF PMSG WIND TURBINE SYSTEM

Parameter	Value
Rated power (P_{rated})	2.7 MW
Rated line voltage (V_{lrated})	3300 V
Rated ac input current (I_{rated})	520 A
Frequency (f_{in})	60 Hz
DC-link voltage (V_{DC})	5200 V
DC-link capacitance (C_{DC})	6 mF
Converter switching frequency (f_{sw})	1020 Hz
Grid side line inductance (L_s)	1.07 mH (0.1 pu)
Transformer leakage inductance (L_{tr})	0.54 mH (0.05 pu)
Filter inductance (L_f)	1.2 mH (0.112 pu)
Filter capacitance (C_f)	0.24 mF (0.365 pu)
Filter resistance (R_f)	0.3 Ω (0.07 pu)

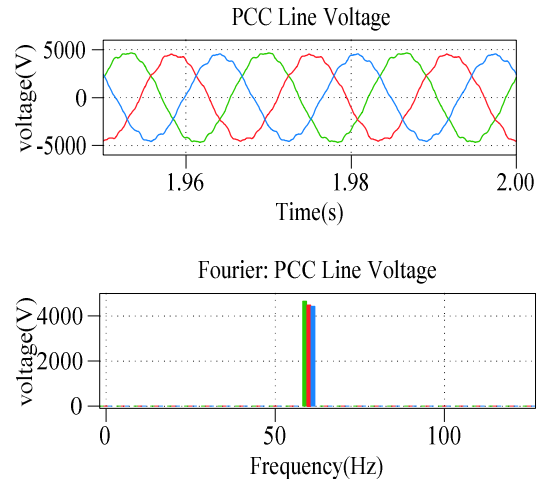


Fig. 8. PCC line voltages without compensation algorithm.

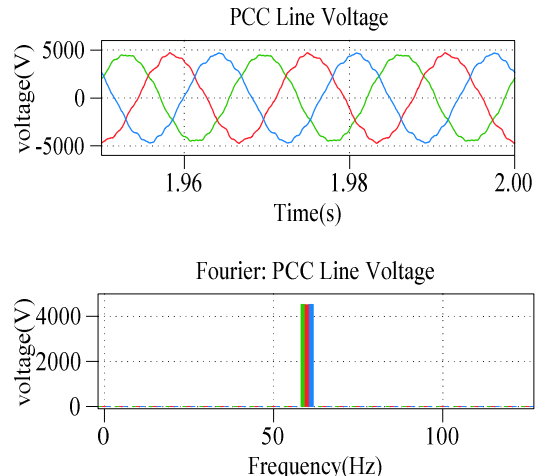


Fig. 9. PCC line voltages with NCI algorithm.

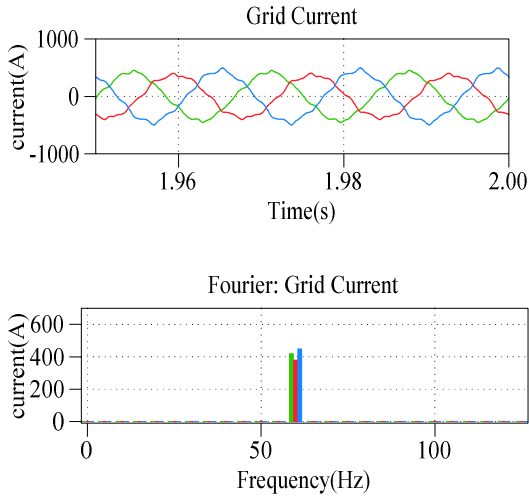


Fig. 10. Grid currents without compensation algorithm.

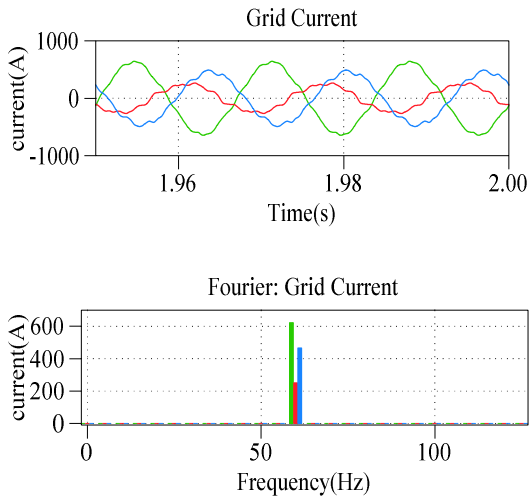


Fig. 11. Grid currents with NCI algorithm.

gives a rise to a larger power loss in switching devices of converter. Therefore, proposed NCI control algorithm may suffer from this increasing loss factor due to additionally injected negative sequential component of input currents. However, as long as the peak current of ac input current having a injected negative sequential component is maintained below the value of rated condition ($735A_{pk}$), the disadvantage of NCI control algorithm doesn't necessarily undermine the system efficiency and requires enlarged cooling system. This operating condition can be satisfied when the wind turbine generates the output power less than the rated power of 2.7MW. For example, operating condition in this paper has the output power generation at 60% of rated value. In general, the mean value of wind speed is below the rated wind speed of 12m/s in a typical off-shore wind turbine.

TABLE IV
COMPARISON OF LINE VOLTAGES AT PCC AND GRID CURRENT (CONDITION : IF=3%, POWER=60%)

Variables	Conventional algorithm	NCI algorithm
PCC line voltage v_{ab}	4663 V_{pk}	4523 V_{pk}
PCC line voltage v_{bc}	4485 V_{pk}	4520 V_{pk}
PCC line voltage v_{ca}	4429 V_{pk}	4533 V_{pk}
IF of PCC voltage	3.1%	0%
Grid current i_a	419 A_{pk}	623 A_{pk}
Grid current i_b	380 A_{pk}	250 A_{pk}
Grid current i_c	449 A_{pk}	466 A_{pk}



Fig. 12. Experiment set-up of 36kW test-bed.

6. Experiment

In general, the unbalanced voltage phenomena becomes more frequent as the stiffness of ac grid is weak, i. e. large value of line inductance. The operating condition chosen for the experimental verification in this paper is set to reflect the worst condition of weak ac grid. The parameters of experiment setup and its operating condition are summarized in TABLE V. Experiment setup to validate the proposed NCI control algorithm is illustrated in Fig. 12.

In Fig. 13-16, the experiment result of proposed NCI control algorithm is described for the operating conditions under IF of 1% and 5% of rated power. The corresponding numerical data are summarized in TABLE VI for the sake of readers' convenience.

TABLE V
PARAMETERS OF EXPERIMENT SETUP

Parameter	Value
Rated power (P_{rated})	36 kW
Rated line voltage (V_{lrated})	460 V
Rated ac input current (I_{rated})	46 A
Frequency (f_{in})	60 Hz
DC link voltage (V_{DC})	858 V
Converter switching frequency (f_{sw})	10 kHz
Grid side line inductance (L_s)	2 mH (0.128 pu)
Transformer leakage inductance (L_{tr})	2 mH (0.128 pu)
Filter inductance (L_f)	0.5 mH (0.064 pu)
DC link capacitance (C_{DC})	1.23 mF

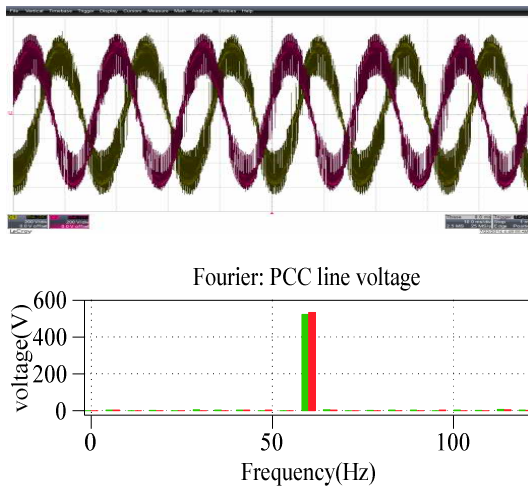


Fig. 13. PCC line voltages without compensation algorithm.

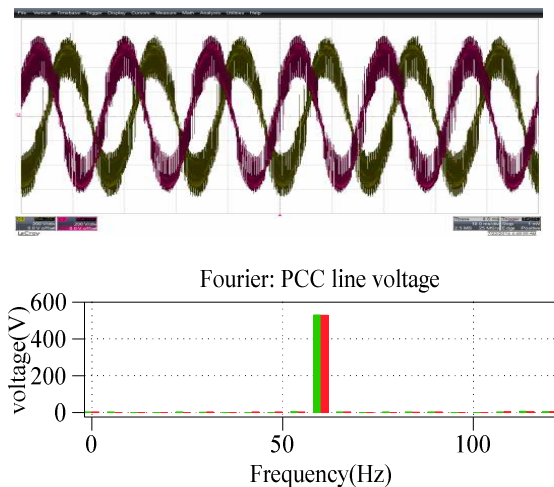


Fig. 14. PCC line voltages with NCI algorithm.

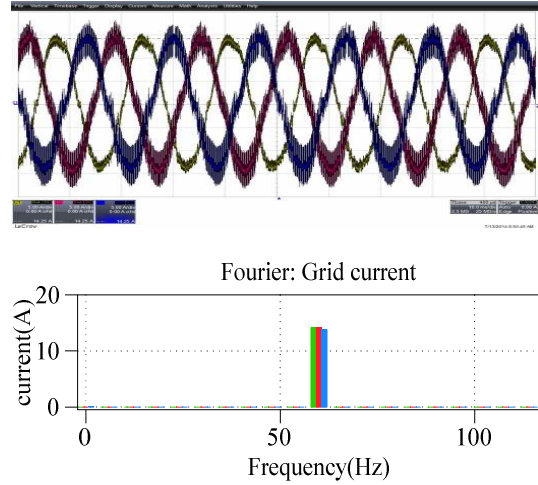


Fig. 15. Grid currents without compensation algorithm.

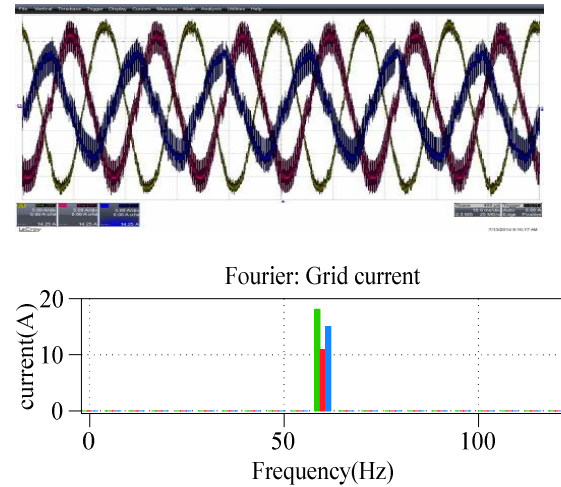


Fig. 16. Grid currents with NCI algorithm.

TABLE VI
COMPARISON OF LINE VOLTAGES AT PCC AND GRID CURRENT (CONDITION : IF=1%, POWER=5%)

Variables	Conventional algorithm	NCI algorithm
PCC line voltage v_{ab}	522 V_{pk}	530 V_{pk}
PCC line voltage v_{bc}	533 V_{pk}	529 V_{pk}
Grid current i_a	14.1 A_{pk}	18 A_{pk}
Grid current i_b	14.1 A_{pk}	10.9 A_{pk}
Grid current i_c	13.7 A_{pk}	15 A_{pk}

As shown in Fig. 14 and TABLE VI, the proposed NCI control algorithm actively compensates for the unbalanced grid voltage. As a result, NCI control algorithm makes the three-phase line voltages at PCC balanced having the IF of almost zero. Fig. 16 shows the waveforms of three-phase ac input currents under the condition with NCI control algorithm considered. It is clearly noted from Fig. 16 that the three-phase ac

input currents become more unbalanced as compared to those of Fig. 15 because of injected negative sequential component of input current. In Fig. 13–16, waveforms verify the fact that NCI control algorithm can improve the voltage quality of PCC voltage at the cost of negative sequence current. Unbalanced input current as illustrated in Fig. 16 due to injected negative sequence can be tolerable in wind turbines as long as the currents are regulated below the rated values such as operating conditions of low wind speed. These are also consistent with the simulation results.

7. Conclusion

This paper investigates the behavior of wind turbine system under the unbalanced PCC voltages and proposes a negative sequence current injection algorithm to actively compensate for voltage imbalance at PCC. The algorithm is to cancel the negative sequential component of voltage by injecting the appropriate negative sequential component of input current. As the depth of imbalance becomes severe, the necessary magnitude of negative sequence current also increases over the current capability of PCS. Under the operating conditions in which unbalanced PCC voltages are rarely generated or negligible, the proposed concept may suffer from the increased loss. However, the proposed concept becomes quite effective where the balancing PCC voltage is an important issue or even a mandatory operating principle to meet the grid code. When the output power of wind turbine gets smaller at low wind speed, the injection of negative sequence current becomes more effective under the current limit of PCS. In a wind farm consisting of multiple wind turbines connected to a collector bus, the contribution of negative sequence current generated by each wind turbine can be summed to compensate for the imbalance at PCC. The proposed control algorithm makes it possible for wind farms to generate a high quality output power under unbalanced grid disturbance.

References

[1] S. Yang, S. Kim, J. Choi, I. Choy, S. Song, S. Lee, and D. Lee, "A compensation of the grid current unbalance and distortion caused by the grid voltage unbalance and distortion in 3-phase bi-directional DC to AC inverter," *The Transactions of the Korean Institute of Power Electronics*, Vol. 18, No. 2, pp. 161–168, Apr. 2013.

This work was supported by the National Research Foundation of Korea (NRF) grant funded by the Korea government (MSIP) (No. 2010-0028509).

This work was supported by the National Research Foundation of Korea (NRF) grant funded by the Korea government (MSIP) (No. 2014R1A2A1A11053678).

Nomenclature

Variables	Definition
v_{gs}	grid side converter voltage
v_s	grid voltage
i_{gs}	grid side converter current
i_s	grid current
L_f, C_f, R_f	filter
L_{tr}	transformer leakage inductance
L_s	grid side inductance
a, b, c	phase of a, b and c
v_{pcc}	PCC voltage
v_f	filter voltage
i_f	filter current
P_{so}	active power
Q_{so}	reactive power
ω	synchronous speed

- [2] Y. Suh and T. A. Lipo, "Control scheme in hybrid synchronous stationary frame for PWM AC/DC converter under generalized unbalanced operating conditions," *IEEE Transactions on Industry Applications*, Vol. 42, No. 3, pp. 825–835, May/June 2006.
- [3] W. Lee, T. Lee, and D. Hyun, "A three-phase parallel active power filter operating with PCC voltage compensation with consideration for an unbalanced load," *IEEE Transactions on Power Electronics*, Vol. 17, No. 5, pp. 807–814, Sep. 2002.
- [4] K. Li, J. Liu, Z. Wang, and B. Wei, "Strategies and operating point optimization of STATCOM control for voltage unbalance mitigation in three-phase three-wire systems," *IEEE Transaction on Power Delivery*, Vol. 22, No. 1, pp. 413–422, Jan. 2007.
- [5] Y. Suh, Y. Go, and D. Rho "A comparative study on control algorithm for active front-end rectifier of large motor drives under unbalanced input," *IEEE Transactions on Industry Applications*, Vol. 47, No. 3, pp. 1419–1431, May/June 2011.
- [6] J. Hu and Y. He, "Modeling and control of grid-connected voltage-sourced converters under generalized unbalanced operation conditions," *IEEE Transactions on Energy Conversion*, Vol. 23, No. 3, pp. 903–913, Sep. 2008.

- [7] H. Song and K. Nam, "Dual current control scheme for PWM converter under unbalanced input voltage conditions," *IEEE Transactions on Industrial Electronics*, Vol. 46, No. 5, pp. 953-959, Oct. 1999.
- [8] A. V. Stankovic and T. A. Lipo, "A novel control method for input output harmonic elimination of the PWM boost type rectifier under unbalanced operating conditions," *IEEE Transactions on Power Electronics*, Vol. 16, No. 5, pp. 603-611, Sep. 2001.
- [9] Y. Abdel-rady, I. Mohamed, and E. F. El-Saadany, "A control scheme for PWM voltage-source distributed-generation inverters for fast load-voltage regulation and effective mitigation of unbalanced voltage disturbances," *IEEE Transactions on Industrial Electronics*, Vol. 55, No. 5, pp. 2072-2084, May 2008.
- [10] M. Savaghebi, A. Jalilian, J.C. Vasquez, and J.M. Guerrero, "Secondary control scheme for voltage unbalance compensation in an islanded droop-controlled microgrid," *IEEE Transactions on Smart Grid*, Vol. 3, No. 2, pp. 797-807, June 2012.
- [11] J. Im, S. Song, and S. Kang, "Analysis and compensation of PCC voltage variations caused by wind turbine power fluctuations," *Journal of Power Electronics*, Vol. 13, No. 5, pp. 854-860, Sep. 2013.



Ja-Yoon Kang

He was born in Korea, in 1986. He received his B.S. in Electrical Engineering from Chonbuk National University, Jeonju, Korea, in 2011, where he is currently working toward his M.S. in Electrical Engineering. His current research interests include the power conversion systems of high power for renewable energy sources and medium electric drive systems.



Dae-Su Han

He was born in Korea, in 1987. He received his B.S. in Electrical Engineering from Chonbuk National University, Jeonju, Korea, in 2013, where he is currently working toward his M.S. in Electrical Engineering. His current research interests include the power conversion systems of high power for renewable energy sources and medium electric drive systems.



Yong-Sug Suh

He was born in Seoul, Korea. He received his B.S. and M.S. in Electrical Engineering from Yonsei University, Seoul, Korea, in 1991 and 1993, respectively, and his Ph.D. in Electrical Engineering from the University of Wisconsin, Madison, WI, USA, in 2004. From 1993 to 1998, he was an Application Engineer in the Power Semiconductor Division of Samsung Electronics Co. From 2004 to 2008, he was a Senior Engineer in the Power Electronics and Medium Voltage Drives Division of ABB,

Turgi, Switzerland. Since 2008, he has been with the Department of Electrical Engineering, Chonbuk National University, Jeonju, Korea, where he is currently an Associate Professor. His current research interests include the power conversion systems of high power for renewable energy sources and medium voltage electric drive systems.



Byoung-Chang Jeong

He was born in Wanju, Korea, in 1976. He received the B.S., M.S., and Ph.D. degrees in Electrical Engineering from Chonbuk National University, Jeonju, Korea, in 1998, 2000, and 2006, respectively. From 2006 to 2009 he was with LG Industrial Systems Company, as a senior research engineer. Since 2009, he has been with the Power & Industrial Systems R&D Center, Hyosung corporation. And he is currently a Chief Researcher. His present research interests are in wind converter and grid connected MW-rating power converter.



Jeong-Joong Kim

He was born in Korea in 1981. He received a B.S. and M.S. degrees in Control & Instrumentation Engineering from Chang-won National University, Chang-won, Korea in 2006 and 2008. From 2006 to 2008 he was with Korea Electro technology Research Institute (KERI), as a research assistant. Since 2008, he has been with the Power & Industrial Systems R&D Center, Hyosung corporation. And he is currently a Senior Researcher. His present research interests are in wind turbine converter.



Jong-Hyoung Park

He was born in Korea in 1979. He received a B.S. degree in Electrical Engineering from Yeungnam University, Kyongsan, Korea in 2006, and a M.S. and a Ph.D. degree in Electrical Engineering from Kyungpook National University, Taegu, Korea in 2008 and 2013, respectively. He is currently work in a HYOSUNG corporation, where he is a Senior Researcher in Power & industrial Systems R&D Center. His current research interests include a grid-connected power conditioning system using renewable energy sources.



Young-Jun Choi

He was born in Korea in 1967. He received a B.S. and a M.S. degrees in Electrical Engineering from Hanyang University, Seoul, Korea in 1991 and 1993, and his Ph.D. degree in Electrical Engineering from Myongji University, Yongin, Korea in 2010, respectively. He has worked for HYOSUNG corporation, Seoul, Korea since 1992, and he is a Office Manager in Power & industrial Systems R&D Center. His current research interests include a grid-connected/off-grid microgrid system using renewable energy sources and energy storage system.